DOE/EH/89321--T1

Final Technical Report:

Improving Measurement Quality Assurance for Photon Irradiations at Department of Energy Facilities

Interagency Agreement # DE-A101-93EH89321

I. Background

For radiation-instrument calibration to be generally acceptable throughout the United States, direct or indirect traceability to a primary standard is required. In most instances, one of the primary standards established at NIST is employed for this purpose. The Department of Energy Laboratory Accreditation Program (DOELAP), carried out at Battelle Pacific Northwest Laboratory (PNL), is an example of a program employing dosimetry based on the NIST primary photon-, beta particle- and neutron-dosimetry standards. [1] The NIST primary dosimetry standards for bremsstrahlung were first established in the 1950s. [2,3] They have been updated since then on several occasions, but the basic bremsstrahlung spectra employed have undergone only few changes. In other countries, bremsstrahlung standards as a rule developed separately, with little or no attempt at international uniformity. However, in the 1970s, Technical Committee 85 of the International Standards Organization (ISO) started its work on establishing sets of internationally acceptable, well-characterized photon beams for the calibration of radiation-protection instruments. [4] This work was based on data obtained by the Gesellschaft für Strahlen- und Umweltforschung (GSF). [5] An additional set of bremsstrahlung beams is added in the present update of ISO 4037. The ISO beams have been widely accepted by ISO Member Nations and also by other international groups, e.g., the International Atomic Energy Agency (IAEA). However, up to now, there have been only minimal attempts in the United States to adopt the internationally accepted calibration beam techniques. This is in contrast to the situation with beta particles and neutrons, where international standards [6,7] are followed in the U.S.

The traditional indifference of the U.S. to international standards did not pose a difficulty in the field of the calibration of radiation-protection instrumentation until the International Commission on Radiation Units and Measurements (ICRU) recommended new operational quantities for use in practical radiation-protection dosimetry [8,9,10], which are to approximate the Equivalent Dose [11] by readily measurable, practical quantities. Inasmuch as the Equivalent Dose is a quantity taking on different values for different photon energies and directions of photon incidence, the conversion coefficients from photon fluence and air kerma to the recommended operational quantities are functions of photon energy and angle of photon incidence. Therefore, instrument calibration in terms of the operational quantities involves a computation of conversion coefficients for the photon beams and the geometry employed in the particular calibration.

Conversion coefficients applicable to the ISO calibration beams and various calibration geometries in practical use are available in the literature. [12,13,14] However, when the committee of the American National Standards Institute (ANSI) revising the standard ANSI N13.11 [15] which is the basis for the National Voluntary Laboratory Accreditation Program

(NVLAP) for dosimetry, decided to require compliance testing in terms of the operational quantities recommended by the ICRU, they had to initiate their own computation of conversion coefficients. [16,17] The reason for this was that the bremsstrahlung beams required for traceability to NIST in most instances are different from the ISO beams.

Similarly, DOELAP, which also desires to express the results of its compliance tests in the future in terms of the applicable operational quantities and has selected NIST beams different from the ones selected for NVLAP, would have to compute its own conversion coefficients. The same procedure would have to be followed by all U.S. organizations interested in using the operational quantities with one or the other of the NIST calibration beams different from the ISO beams.

All these special laborious computations could be avoided if NIST were able to offer the ISO photon beams, since for these, as stated above, conversion coefficients are available in the literature. Recently, DOE was the first government agency to propose that NIST add ISO beams to its standard beams, and subsequently gave NIST a detailed list of the ISO beams that would be desirable to DOELAP.

In addition to the selected NIST bremsstrahlung techniques, DOELAP tests personnel dosimeter performance using K-fluorescence spectra. These spectra are required because of needs peculiar to DOE facilities. Recent improvements in the PNL K-fluorescence facility [18] have called into question the validity of the conversion coefficients that are currently used for these techniques. [19] At present, these fluorescence techniques are not offered at NIST which leaves DOE without the ability to have traceability to a national standard in this area. A proposed solution to this dilemma is to use the ISO narrow spectra and ^{241}Am to approximate the 17- and 59-keV fluorescence beams currently specified by the DOELAP standard.

Finally, there are no well-documented techniques for establishing the equivalence of photon irradiations from facility to facility within DOE as well as from NIST. The lack of detailed procedures for demonstrating such equivalence leave undiscovered subtle variations in photon beams used for calibrations performed in different DOE facilities.

II. Comparison of Current NIST Techniques and ISO 4037 Techniques

It is the intent in this section to make a detailed comparison between the current NIST and the most up-to-date ISO techniques [20]. At present, 41 bremsstrahlung techniques are specified in ISO 4037 while NIST supports a total of 32 techniques. In the following tables, a system of notation has been adopted for the ISO techniques. The prefix "NS" refers to the ISO Narrow Spectrum Series, "WS" refers to the ISO Wide Spectrum Series, "HK" refers to the ISO High Air Kerma Rate Series, and "LK" refers to the ISO Low Air-Kerma Rate Series. For NIST techniques, "H" refers to the NIST Heavily Filtered Series, "M" refers to the NIST Moderately Filtered Series, "L" refers to the NIST Lightly Filtered Series, and "S" refers to the NIST Special Filtered Series. In each case, the number following the series type indicates the tube potential in kV to be employed.

What is evident from the table is that there is already some congruence between NIST and ISO, mainly between the NIST Heavily Filtered (H) techniques and the ISO Narrow Spectrum (NS) techniques at 10, 15, 20, 30, 40, 60, 100 and 300 kV. Also there is near agreement between the NIST Moderately Filtered (M) techniques and the ISO High Air-Kerma Rate (HK) techniques at 30 and 200 kV. In addition, NIST technique M300 is identical to the 300-kV ISO Wide Spectrum (WS) technique. Given these existing equivalences, it makes sense to try to extend the NIST techniques to cover more of the ISO Narrow Spectrum and High Air-Kerma Rate Series. These extensions will also allow the possibility for use of ISO beam techniques in future revisions of the DOELAP standard, which has been suggested by DOE. To this end, NIST was funded by DOE to procure material and make adaptions to the existing NIST x-ray calibration ranges to allow NIST to have the capability of producing all the ISO bremsstrahlung techniques. The following sections describe the steps that were taken to achieve this.

III. Filter Material Acquisition

Specifications for filter materials for producing the ISO bremsstrahlung radiations were prepared and invitations to bid were sent to 34 possible vendors. The specifications were for 10 cm x 10 cm (nominal 4 in. by 4 in.) plates of various thicknesses, having purities of 99.9% or better. Cost analyses was performed on eleven positive respondents resulting in one low bidder for the Pb (Goodfellow[1]), the Sn (Arconium), and for both the Al and Cu (Electronic Space Products International). Samples of material were requested from these vendors to ascertain that a) the required purity and b) the proper transmission uniformity (i.e. lack of crystalline structure which would produce non-uniform x-ray transmission) would be met. Material was ordered from these vendors with thicknesses selected such that combinations could be used to obtain thicknesses required for the ISO techniques. The material ordered is shown in Table 4.

Each 10 x 10 cm filter piece was assigned an identification number consisting of the element followed by a two-digit number. This identification was affixed to the lower left corner of each sample using gummed labels, and remained on the samples throughout the characterization process described below.

IV. Filter Material Characterization: Thickness

Thicknesses of all 228 foil samples were measured at five positions in the NIST shops, using a Mitutoyo BHN710 Coordinate Measuring Machine. Several of the samples were also measured with a micrometer, and the Mitutoyo DGS-E thickness gauge used by the Ionizing Radiation Division to measure film thicknesses. These latter measurements were in agreement to within 10 μm with those of the NIST shops. The thicknesses at the five positions measured in the NIST shops were averaged and used as nominal foil thicknesses for the purpose of combining foils to

[1] Certain commercial manufacturers and products are mentioned in this report by name. This is for informational purposes only and does not imply that these are the best or only providers of the materials or services mentioned, nor does it imply either NIST or DOE indorsement.

come up with the 55 particular thicknesses required to produce filter packs for the 41 ISO bremsstrahlung techniques. All required thicknesses were generated successfully through combinations of the available foils. It was necessary, however, to reduce the thickness of some of the 1-mm Sn plates by about 0.03 to 0.07 mm. This was accomplished by rolling out about half of the plates to under 1 mm for combination with other thicker plates to make the required thicknesses for the ISO techniques. The Sn filters which were rolled out to under 1 mm were again measured in the NIST shops and successfully matched to other filters above 1-mm thickness to achieve the thicknesses required for the ISO beams. All required thicknesses were achieved to less than 5%. Further differences in required Al will be made up when additional Al is added to achieve the 4-mm Al equivalent inherent filtration required by ISO 4037 for the higher energy techniques. The measured thickness and standard deviations of the five measurements are shown in Table 5.

V. Filter Material Characterization: Purity

Samples of all four of the filter elements were analyzed by NIST personnel using x-ray fluorescence (XRF) analysis. There is evidence of some contamination in the Al and the Sn material. The Al contamination (mainly Fe) is well below the level specified in ISO 4037 (99.9%). The Sn contamination is mainly Bi and Pb. The details of the spectral analysis used to determine the metal purity is described below.

Because of the expected purity of the material (99.8+%) and the needed sensitivity of the analysis (parts per thousand), x-ray fluorescence analysis was chosen. A nearly monoenergetic beam of x-rays from a fluoresced secondary target is used to excite characteristic x-ray emission from elements in the sample being analyzed. These x-rays are detected with a high-resolution photon detector for identification and quantification. For the analyses of these 100-mm x 100-mm samples, a Kevex x-ray emission spectrometer system was used, which allowed the entire sample to be inserted on the device. An area of about 0.1 cm^2 was actually in the x-ray beam for analysis. For most of the material analyzed, a Ag secondary target was used, excited with 40-kV bremsstrahlung at tube currents of 0.4, 1.0, or 2.0 mA. Photon spectra from the sample were acquired with the built-in Si(Li) detector and pulse-height analyzer. Peak areas were determined by fitting the region of interest with gaussian functions using Tablecurve Version 3; these were integrated using Simpson's Rule. Background was determined from a straight line drawn between the two ends of gaussian function; the area under this line was subtracted to yield the peak area. An example of one of the fitted peaks is shown in Fig. 1.

The effect of the matrix upon the measured peak was handled in the following manner. First it was assumed that the material was homogeneous, ie. that small amounts of contaminants were uniformly distributed within the bulk volume of the sample. The x-ray flux emitted from contaminant c, in an infinitesimal thickness of sample material, dt, at a depth t in the sample, $\phi_c(t)$, is proportional to the amount of contaminant per unit area, m_c and to the flux of fluorescent x-rays of energy E_i penetrating the sample to depth t, $\phi_i(t,E)$. Thus for any depth t we have

$$\phi_c(t) = K_c\, m_c\, \phi_i(t,E_i) = K_c\, m_c\, \phi_i(E_i) e^{-\rho t \cos(45°)\mu(Ei)/\rho} \qquad \text{Eq. 1}$$

where $\phi_i(E_i)$ is the flux of fluorescence x-rays incident at the surface of the sample, $\mu(E_i)/\rho$ is the linear attenuation coefficient of photons of energy E_i in material of density ρ, cos(45°) is a factor to account for the source/detector geometry, and K_c is the constant of proportionality, which depends upon the photo-ionization cross section of the contaminant element.

The signal reaching the detector from the fluoresced contaminant emitting characteristic x-rays of energy E_c at depth t, $\Phi_c(t)$, is given by

$$\Phi_c(t) = \phi_c(t) e^{-\rho t \cos(45°)\mu(Ec)/\rho} \qquad \text{Eq. 2}$$

where $\mu(E_c)/\rho$ is the linear attenuation coefficient of photons on energy E_c in material of density ρ, and again cos(45°) is a factor to account for detector geometry. The total signal reaching the detector from the fluoresced sample is the integrated sum of all the layers of the sample, Φ_c, given by

$$\Phi_c = \int_0^T \Phi_c(t)\, dt = K_c\, m_c\, \phi_i(E_i) \int_0^T e^{-\rho t \cos(45°)[(\mu(Ei)/\rho)+(\mu(Ec)/\rho)]}\, dt \qquad \text{Eq. 3}$$

where T is the sample thickness. The quantity $K_c\phi_i(E_i)$ is characteristic of the contaminant, the secondary target material, and the tube current. It is established by analyzing a sample of known composition in the same geometry as the unknown sample. Knowing this quantity from the system calibration (described below), it is possible to determine the unknown amount of contamination, m_c, from the measured peak area. The matrix effect integral can be evaluated as

$$M_c = (\rho T \cos(45°)[(\mu(E_i)/\rho)+(\mu(E_c)/\rho)])^{-1} (1-e^{-\rho T \cos(45°)[(\mu(Ei)/\rho)+(\mu(Ec)/\rho)]}) \qquad \text{Eq. 4}$$

The linear attenuation coefficients were calculated for the materials and energies of interest using the program XCOM, written by John Hubbel.

The system was calibrated by analyzing a sample (#927) which consists of a 10-cm^2 glass disk of total mass 1.616 mg, with by weight 9.13% Pb, 9.46% Fe and 2.24% Zn. This sample was analyzed using the Ag secondary target and the three beam currents employed on the unknowns. The K_α line was used for the Fe and Zn contaminants, while the L_α line was used for Pb. Table 6 summarizes the measurements using this sample.

To account for the matrix effect as described above it was necessary to calculate the exact fraction by weight of each elemental component of this sample. Since the known contaminants were in the form of oxides (Fe_2O_3, ZnO and PbO) in an SiO_2 matrix, O was the dominant component. The calculated weights and weight fractions for this sample are given in Table 7.

The sample density was calculated as a weighted average of the densities of the four oxide components, SiO_2 (ρ=2.32 g/cm^3, 73.85%), Fe_2O_3 (ρ=5.24 g/cm^3, 13.53%), PbO (ρ=9.53 g/cm^3, 9.83%) and ZnO (ρ=5.47 g/cm^3, 2.79%), yielding a bulk density of the sample of 3.51

g/cm^3. Given the known area and total mass, this density implies a sample thickness of 46 μm. The constituents and weight fractions of Table 2 were input to the program XCOM to get the linear attenuation coefficients for this material at the energies of interest; the attenuation coefficient for the Ag fluorescence x-rays, whose energy was taken as 22.0 keV, was also calculated. The values shown in Table 8 are those for total attenuation without coherent scattering. Applying these coefficients, the known mass concentrations in Sample 927, and the measured counts for Ag excitation for the three beam currents, the following calibration constants are obtained using Eqs. 3 and 4. Altogether, 5 samples were analyzed for purity. Two of the samples, Pb and Cu, showed no detectable contamination and are not further discussed. The other three samples showed some contamination; these samples are described in Table 10.

Each sample (except Sn #18) was analyzed twice, with different sides facing the source and detector. The sample designations, elements detected, measured counts (in 300 seconds) are shown in Table 11. Material purity was calculated from the matrix mass density as $100*(m_c+\rho/\rho)$. Note that the system calibration factor for Zn was used to quantify the unknown amount of Cu, since they are sufficiently close to each other in atomic number for small differences in the ionization cross section to be nearly negligible.

VI. Filter Material Characterization: X-Ray Transmission Uniformity

Although there are no specifications for filter transmission uniformity, this parameter is of concern because of possible crystalline structure in purer materials which would allow preferential transmission along crystal axes. This effect has been observed in pure samples of Sn [21]. To avoid this problem, the material must be specified to be "well worked", to homogenize crystals as much as possible. Samples of the filter material were examined for x-ray transmission uniformity using conventional x-ray radiography and high-resolution densitometric techniques prior to being mounted in the filter wheels. A 110 kV cabinet x-ray unit was employed for this purpose with the sample mounted 32 cm from the x-ray tube window. The sample was placed on a 9.2-cm diameter Pb aperture to define an imaging area. Type M radiographic film was placed at 75.7 cm from the tube window which resulted in a magnification factor of 2.33. The filters examined are shown in Table 12, and an example of a densitometric scan is shown in Figure 2. The inset histogram in this figure indicates two density peaks, the main one at density 1.56, and a smaller one at 1.545. The contours shown on this plot are at densities of 1.45 and 1,545. They show that the smaller peak is associated with the lower and left sides of the filter area. The difference in transmission between these two areas ($<1\%$) is the same as the thickness variation of this sample as indicated in Table 5b.

VII. Design of Removable Filter Wheel System

Preliminary designs for new filter holders were considered, with the goal being to implement as many of the ISO techniques as possible while still maintaining (for the time being) the current NIST techniques. To accomplish this, multiple filter wheel designs were necessary. Preliminary designs were prepared by the NIST Fabrication Technology Division for 16-position removable 76-cm diameter filter wheels. The design goals were for 3" apertures allowing larger field sizes

than are available in the current 2" diameter NIST filters. The removable wheel design is deemed the most flexible and open ended for allowing future implementation of more techniques as the need arises. The final design prepared by the NIST Fabrication Technology Division utilized 8-position removable filter wheels with 3½" apertures, with total wheel diameters of 49 cm. The smaller size was chosen so that modifications to the existing support structures would be kept to a minimum. The wheels are center driven with motorized worm-gear rotary tables using high-torque stepping motors, and precision optical disk encoders for positive position sensing. The motors are controlled with Compumotor 4000 motion controllers, and control programs were written to select filter and aperture positions from relatively simple input parameters from the host computer. Final design and construction of the rotary table supports for both x-ray sets (100-kV and 400-kV) was completed in Fall 1995.

VIII. Filter Installation

Table 13 shows the arrangement of the material samples used to arrive at the thicknesses needed to achieve the ISO filtrations. Each position on each of the five ISO wheels was labeled both with a human-readable as well as a bar-code label. American Microsystem Model 2000 and 2500 laser bar-code scanners were mounted over both filter and aperture wheels on each set for additional position verification, as well as for verifying that the proper wheel is mounted.

IX. References

[1] "Department of Energy Standard for the Performance Testing of Personnel Dosimetry Systems", DOE/EH-0027, U.S. Department of Energy, Washington, D.C. (December 1986).

[2] Lamperti, P.J., T.P. Loftus and R. Loevinger, "Calibration of x-ray and gamma-ray instruments", NBS Special Publication 250-16, U.S. Department of Commerce, Washington, D.C. (March 1988).

[3] "NIST Calibration Services Users Guide 1991", Simmons, J.D. ed., NIST Special Publication 250, U.S. Department of Commerce, Washington, D.C. (March 1991).

[4] "X and Gamma Reference Radiations for Calibrating Dosemeters and Dose Ratemeters and for Determining their Response as a Function of Photon Energy", International Standards Organization Standard 4037 (1983).

[5] Seelentag, W.W., W. Panzer, G. Drexler, L. Platz and F. Santer, "A Catalog of Spectra for the Calibration of Dosemeters", GSF Bericht S 560, Gesellschaft für Strahlen- und Umweltforschung, Munich (March 1979).

[6] "Reference Beta Radiations for Calibrating Dosemeters and Doseratemeters and for Determining their Response as a Function of Beta Radiation Energy," International Standards Organization Standard 6980 (July 1984).

[7] "Neutron Reference Radiations for Calibrating Neutron-Measuring Devices used for Radiation Protection Purposes and for Determining their Response as a Function of Neutron Energy," International Standards Organization Standard 8529 (October 1989).

[8] "Determination of Dose Equivalents Resulting from External Radiation Sources", ICRU Report 39, International Commission on Radiation Units and Measurements, Bethesda, MD (February 1985).

[9] "Determination of Dose Equivalents Resulting from External Radiation Sources - Part 2", ICRU Report 43, International Commission on Radiation Units and Measurements, Bethesda, MD (December 1988).

[10] "Measurement of Dose Equivalents from External Photon and Electron Radiations", ICRU Report 47, International Commission on Radiation Units and Measurements, Bethesda, MD (April 1992).

[11] "1990 Recommendations of the International Commission on Radiological Protection", ICRP Publication 60, Annals of the International Commission on Radiological Protection, Pergamon Press, Oxford (1991).

[12] Grosswendt, B., "Conversion Coefficients for Calibrating Individual Photon Dosemeters in Terms of Dose Equivalents Defined in an ICRU Tissue Cube and PMMA Slabs," Radiat. Prot. Dosim. **32**, 219-231 (1990).

[13] Grosswendt, B., "The Angular Dependence and Irradiation Geometry Factor for the Dose Equivalent for Photons in Slab Phantoms of Tissue-Equivalent Material and PMMA," Radiat. Prot. Dosim. **35**, 221-235 (1991).

[14] Grosswendt, B., "Coefficients for the Conversion of Air-Collision-Kerma to Dose-Equivalent for the Calibration on Individual Dosemeters in X-Ray Fields," Radiat. Prot. Dosim. **40**, 169-183 (1992).

[15] "American National Standard for Dosimetry - Personnel Dosimetry Performance - Criteria for Testing," ANSI N13.11, American National Standards Institute, New York (1983).

[16] Zeman, G. H., C. G. Soares and R. T. Devine, "Why Change the X-Ray Conversion Factors in ANSI N13.11?," Proceedings of the 3rd Conference on Radiation Protection and Dosimetry, Oak Ridge National Laboratory, Oak Ridge, TN (October 1991).

[17] Soares, C. G. and P. R. Martin, "A Consistent Set of Conversion Coefficients for Personnel and Environmental Dosimetry", Proceedings of the Panasonic User's Group Meeting, Somerset, PA, June 5-9, 1995.

[18] Fox, R. A., R. T. Hogan, C. D. Hooker and J. C. McDonald, "An Improved Method for the Generation of K-Fluorescence X-Rays," unpublished report from Battelle-Pacific Northwest Laboratories (1989).

[19] Yoder, R. C., W. T. Bartlett, J. W. Courtney, C. D. Hooker, J. A. Holland and B. T. Hogan, "Confirmation of Conversion Factors Relating Exposure and Dose-Equivalent Index Presented in ANSI N13.11," NUREG/CR-1037, PNL-3219, Pacific Northwest Laboratory, Richland, WA (November 1979).

[20] "X and Gamma Reference Radiations for Calibrating Dosemeters and Dose Ratemeters and for Determining their Response as a Function of Photon Energy Part 1 - Characteristics of the Radiations and their Methods of Production", draft of revised International Standards Organization Standard 4037 (September 1991).

[21] Kramer, H.M., Physikalisch-Technische Bundesanstalt (PTB), private communication, 1993.

Table 1. Comparison of ISO and NIST Bremsstrahlung Techniques Below 50 kV

Beam Code	Inherent Filtration, mm	Added Filtration, mm				Half-Value Layer, mm	
		Al	Cu	Sn	Pb	Al	Cu
L10	1 Be					0.029	
HK10	4 Be					0.036	
NS10	1 Be	0.1				0.047	
H10	1 Be	0.105				0.048	
LK10	1 Be	0.3				0.058	
L15	1 Be					0.050	
NS15	1 Be	0.5				0.14	
H15	1 Be	0.5				0.152	
L20	1 Be					0.071	
HK20	4 Be	0.15				0.12	
M20	1 Be	0.23				0.152	
NS20	1 Be	1.0				0.32	
H20	1 Be	1.021				0.36	
LK20	1 Be	2.0				0.42	
NS25	1 Be	2.0				0.66	
L30	1 Be	0.265				0.22	
M30	1 Be	0.50				0.36	
HK30	4 Be	0.52				0.38	
NS30	1 Be	4.0				1.15	
H30	1 Be	4.13				1.23	
LK30	1 Be	4.0	0.18			1.46	
LK35	1 Be		0.25			2.20	
L40	1 Be	0.50				0.49	
M40	1 Be	0.786				0.73	
NS40	4 Al		0.21				0.084
H40	1 Be	4.05	0.26			2.9	0.093

Table 2. Comparison of ISO and NIST Bremsstrahlung Techniques Between 50 and 125 kV

Beam Code	Inherent Filtration, mm	Added Filtration, mm				Half-Value Layer, mm	
		Al	Cu	Sn	Pb	Al	Cu
L50	1 Be	0.639				0.75	
M50	1 Be	1.021				1.02	0.032
H50	3 Be	4.0			0.10	4.2	0.142
LK55	4 Al		1.2				0.25
M60	3 Be	1.51				1.68	0.052
HK60	4 Be	3.2				2.42	0.079
S60	3 Be	4.0				2.8	0.089
WS60	4 Al		0.3				0.18
NS60	4 Al		0.6				0.24
H60	3 Be	4.0	0.61			6.0	0.24
LK70	4 Al		2.5				0.49
S75	1 Be	1.504				1.86	
L80	1 Be	1.284				1.83	
WS80	4 Al		0.5				0.35
NS80	4 Al		2.0				0.58
L100	1 Be	1.978				2.8	
HK100	4 Be	3.9	0.15			6.56	0.30
M100	3 Be	5.0				10.2	0.67
NS100	4 Al		5.0				1.11
H100	3 Be	4.0	5.2			13.5	1.14
LK100	4 Al		0.5	2.0			1.24
WS110	4 Al		2.0				0.96
NS120	4 Al		5.0	1.0			1.71
LK125	4 Al		1.0	4.0			2.04

Table 3. Comparison of ISO and NIST Bremsstrahlung Techniques Above 125 kV

Beam Code	Inherent Filtration, mm	Added Filtration, mm				Half-Value Layer, mm	
		Al	Cu	Sn	Pb	Al	Cu
M150	3 Be	5.0	0.25			10.2	0.67
WS150	4 Al		2.0	1.0			1.86
NS150	4 Al			2.5			2.36
H150	3 Be	4.0	4.0	1.51		17.0	2.5
LK170	4 Al		1.0	3.0	1.5		3.47
M200	3 Be	4.1	1.12			14.9	1.69
HK200	4 Al		1.15			14.7	1.70
WS200	4 Al			2.0			3.08
NS200	4 Al		2.0	3.0	1.0		3.99
H200	3 Be	4.0	0.60	4.16	0.77	19.8	4.1
LK210	4 Al		0.5	2.0	3.5		4.54
LK240	4 Al		0.5	2.0	5.5		5.26
HK250	4 Al		1.6			16.6	2.47
M250	3 Be	5.0	3.2			18.5	3.2
WS250	4 Al			4.0			4.22
NS250	4 Al			2.0	3.0		5.19
H250	3 Be	4.0	0.60	1.04	2.72	22	5.2
HK280	4 Al		3.0			18.6	3.37
HK300	4 Al		2.5			18.7	3.40
WS300	4 Al			6.5			5.20
M300	3 Be	4.0		6.5		22	5.3
NS300	4 Al			3.0	5.0		6.12
H300	3 Be	4.1		3.0	5.0	23	6.2

Table 4. Material Acquired for ISO Filters

Element	Thickness, mm	Number Ordered
Pb	2.00	10
Pb	1.00	10
Pb	0.50	5
Pb	0.10	10
Sn	1.00	38
Sn	0.50	2
Cu	1.00	20
Cu	0.50	21
Cu	0.15	10
Cu	0.10	20
Cu	0.01	10
Al	2.00	10
Al	1.00	10
Al	0.50	10
Al	0.10	21
Al	0.05	20

Table 5a: Measured Thicknesses of Filter Samples

#	t, mm	SD, mm	#	t, mm	SD, mm	#	t, mm	SD, mm	#	t, mm	SD, mm
Pb01	1.9259	0.0098	Pb20	0.9814	0.0205	Sn04	1.0740	0.0081	Sn23	1.0802	0.0072
Pb02	1.9149	0.0055	Pb21	0.4826	0.0195	Sn05	1.0690	0.0062	Sn24	1.0680	0.0798
Pb03	1.9103	0.0147	Pb22	0.4867	0.0144	Sn06	1.0630	0.0048	Sn25	1.0664	0.0042
Pb04	1.9130	0.0033	Pb23	0.4817	0.0277	Sn07	1.0682	0.0095	Sn26	1.0973	0.0113
Pb05	1.9258	0.0125	Pb24	0.4804	0.0337	Sn08	1.0664	0.0075	Sn27	1.0666	0.0073
Pb06	1.9324	0.0173	Pb25	0.4859	0.0266	Sn09	1.0764	0.0116	Sn28	1.0755	0.0123
Pb07	1.9321	0.0041	Pb26	0.1263	0.0039	Sn10	0.9545	0.0179	Sn29	1.0583	0.0235
Pb08	1.9252	0.0132	Pb27	0.1243	0.0013	Sn11	0.9481	0.0154	Sn30	1.0639	0.0252
Pb09	1.9344	0.0081	Pb28	0.1251	0.0015	Sn12	0.9446	0.0121	Sn31	0.9533	0.0240
Pb10	1.9225	0.0058	Pb29	0.1246	0.0032	Sn13	0.9178	0.0015	Sn32	0.9315	0.0250
Pb11	0.9716	0.0197	Pb30	0.1221	0.0048	Sn14	0.9603	0.0178	Sn33	0.9477	0.0076
Pb12	1.0224	0.0113	Pb31	0.1213	0.0013	Sn15	0.9165	0.0178	Sn34	0.9360	0.0163
Pb13	0.9955	0.0079	Pb32	0.1228	0.0015	Sn16	0.9415	0.0160	Sn35	0.9663	0.0139
Pb14	1.0403	0.0190	Pb33	0.1302	0.0078	Sn17	0.9446	0.0153	Sn36	0.9407	0.0187
Pb15	1.0106	0.0085	Pb34	0.1233	0.0021	Sn18	0.9461	0.0271	Sn37	0.9934	0.0412
Pb16	1.0478	0.0215	Pb35	0.1249	0.0027	Sn19	0.9592	0.0262	Sn38	0.9136	0.0396
Pb17	0.9759	0.0083	Sn01	1.0628	0.0030	Sn20	0.9663	0.0127	Sn39	0.4841	0.0209
Pb18	1.0030	0.0041	Sn02	1.0375	0.0166	Sn21	1.0754	0.0073	Sn40	0.4935	0.0141
Pb19	1.0184	0.0066	Sn03	1.0299	0.0189	Sn22	1.0684	0.0113	Cu01	1.0186	0.0016

Table 5b: Measured Thicknesses of Filter Samples

#	t, mm	SD, mm	#	t, mm	SD, mm	#	t, mm	SD, mm	#	t, mm	SD, mm
Cu02	1.0184	0.0008	Cu21	0.5245	0.0059	Cu40	0.5260	0.0059	Cu59	0.1027	0.0033
Cu03	1.0208	0.0011	Cu22	0.5274	0.0032	Cu41	0.5285	0.0061	Cu60	0.1022	0.0035
Cu04	1.0142	0.0007	Cu23	0.5261	0.0073	Cu42	0.1851	0.0396	Cu61	0.1195	0.0401
Cu05	1.0151	0.0011	Cu24	0.5276	0.0066	Cu43	0.1356	0.0054	Cu62	0.1050	0.0054
Cu06	1.0238	0.0014	Cu25	0.5289	0.0046	Cu44	0.1322	0.0064	Cu63	0.1010	0.0015
Cu07	1.0247	0.0011	Cu26	0.5337	0.0091	Cu45	0.1392	0.0099	Cu64	0.1008	0.0012
Cu08	1.0238	0.0013	Cu27	0.5331	0.0038	Cu46	0.1315	0.0067	Cu65	0.0998	0.0021
Cu09	1.0197	0.0013	Cu28	0.5331	0.0087	Cu47	0.1294	0.0026	Cu66	0.0993	0.0020
Cu10	1.0206	0.0029	Cu29	0.5314	0.0057	Cu48	0.1317	0.0050	Cu67	0.0989	0.0028
Cu11	1.0193	0.0013	Cu30	0.5336	0.0079	Cu49	0.1342	0.0058	Cu68	0.0978	0.0019
Cu12	1.0186	0.0009	Cu31	0.5297	0.0081	Cu50	0.1320	0.0027	Cu69	0.0975	0.0013
Cu13	1.0241	0.0155	Cu32	0.5321	0.0163	Cu51	0.1347	0.0046	Cu70	0.1007	0.0071
Cu14	1.0180	0.0017	Cu33	0.5298	0.0033	Cu52	0.1058	0.0029	Cu71	0.0990	0.0026
Cu15	1.0183	0.0008	Cu34	0.5290	0.0056	Cu53	0.1018	0.0011	Cu72	0.0125	0.0005
Cu16	1.0195	0.0017	Cu35	0.5316	0.0121	Cu54	0.1035	0.0040	Cu73	0.0125	0.0007
Cu17	1.0134	0.0009	Cu36	0.5291	0.0081	Cu55	0.1026	0.0025	Cu74	0.0127	0.0006
Cu18	1.0144	0.0003	Cu37	0.5313	0.0045	Cu56	0.1077	0.0058	Cu75	0.0128	0.0009
Cu19	1.0232	0.0008	Cu38	0.5278	0.0044	Cu57	0.1048	0.0041	Cu76	0.0130	0.0011
Cu20	1.0220	0.0008	Cu39	0.5271	0.0047	Cu58	0.1037	0.0050	Cu77	0.0125	0.0005

Table 5c: Measured Thicknesses of Filter Samples

#	t, mm	SD, mm	#	t, mm	SD, mm	#	t, mm	SD, mm	#	t, mm	SD, mm
Cu78	0.0126	0.0009	Al15	1.0566	0.0049	Al34	0.1046	0.0077	Al53	0.0510	0.0005
Cu79	0.0122	0.0004	Al16	1.0453	0.0052	Al35	0.0996	0.0024	Al54	0.0509	0.0003
Cu80	0.0123	0.0007	Al17	1.0523	0.0033	Al36	0.1005	0.0025	Al55	0.0511	0.0007
Cu81	0.0122	0.0003	Al18	1.0446	0.0062	Al37	0.0975	0.0007	Al56	0.0502	0.0004
Cu82	0.5184	0.0068	Al19	1.0632	0.0045	Al38	0.1031	0.0104	Al57	0.0507	0.0002
Al01	2.0409	0.0012	Al20	1.0706	0.0048	Al39	0.0982	0.0016	Al58	0.0509	0.0003
Al02	2.0409	0.0009	Al21	0.5336	0.0225	Al40	0.1019	0.0070	Al59	0.0511	0.0003
Al03	2.0482	0.0021	Al22	0.5298	0.0091	Al41	0.0980	0.0034	Al60	0.0507	0.0004
Al04	2.0502	0.0248	Al23	0.5283	0.0108	Al42	0.0981	0.0025	Al61	0.0507	0.0006
Al05	2.0470	0.0009	Al24	0.5326	0.0149	Al43	0.1069	0.0119	Al62	0.0504	0.0003
Al06	2.0400	0.0009	Al25	0.5464	0.0135	Al44	0.0961	0.0012	Al63	0.0504	0.0003
Al07	2.0386	0.0014	Al26	0.5201	0.0117	Al45	0.0966	0.0010	Al64	0.0507	0.0004
Al08	2.0409	0.0019	Al27	0.5227	0.0113	Al46	0.0974	0.0018	Al65	0.0508	0.0002
Al09	2.0412	0.0016	Al28	0.5408	0.0083	Al47	0.0984	0.0024	Al66	0.0501	0.0004
Al10	2.0419	0.0010	Al29	0.5110	0.0049	Al48	0.0974	0.0022	Al67	0.0503	0.0002
Al11	1.0525	0.0038	Al30	0.5155	0.0048	Al49	0.0969	0.0012	Al68	0.0495	0.0004
Al12	1.0546	0.0062	Al31	0.0992	0.0019	Al50	0.0990	0.0014	Al69	0.0498	0.0005
Al13	1.0599	0.0047	Al32	0.1017	0.0028	Al51	0.1029	0.0084	Al70	0.0503	0.0005
Al14	1.0681	0.0065	Al33	0.0997	0.0016	Al52	0.0509	0.0004	Al71	0.0502	0.0004

Table 6. Measured Net Peak Areas for Sample 927 with 40 kV on Ag Secondary for 300 sec

Element	Photon Energy (keV)	Net Peak Areas		
		0.4 mA	1.0 mA	2.0 mA
Fe	6.40	1506	3322	6414
Zn	8.63	693	1507	3081
Pb	10.53	2361	5457	10362

Table 7. Elemental Constituency of Calibration Sample 927

Element	Atomic Weight	Amount in Sample 927	
		Mass, mg	Weight Fraction
O	15.9994	0.7215	0.4465
Si	28.09	0.5579	0.3452
Fe	55.85	0.1529	0.0946
Pb	207.19	0.1475	0.0913
Zn	65.37	0.0362	0.0224

Table 8. Linear Attenuation Coefficients from XCOM for Energies and Materials of Interest

Element	Energy (keV)	Linear Attenuation Coefficient (cm^2/g) in		
		Sample 927	Al	Sn
Fe	6.40	96.5	94.9	--
Cu	8.0	--	49.6	--
Zn	8.63	63.1	--	--
Pb	10.53	40.6	--	118
Ag	22	9.79	2.45	15.5

Table 9. Calibration Constants Using 40kV Excitation of Ag Secondary Target for 300 sec

Element	Mass Concentration, m_c ($\mu g/cm^2$)	Matrix Effect, M_c	Calibration Constant, $[K_c\phi_i(E_i)]^{-1}$ (ng cm^{-2} ct^{-1})		
			0.4 mA	1.0 mA	2.0 mA
Fe	15.29	0.376	3.81	1.73	0.895
Zn	3.62	0.487	2.55	1.17	0.572
Pb	14.75	0.594	3.71	1.61	0.846

Table 10. Sample Description and Analysis Conditions

Sample Designation	Thickness, T (cm)	Density, ρ (g/cm^3)	Excitation Current, (mA)
Sn #18	0.1104	7.28	0.4
Sn #39	0.04841	7.28	0.4
Sn #40	0.04935	7.28	2.0
Al #21	0.05336	2.70	1.0

Table 11: Measured Sample Purities

Sample Designation	Detected Contaminant	Measured Counts	Matrix Effect, M_c	Mass Concentration, m_c ($\mu g/cm^2$)	Material Purity (%)
Sn #18	Pb	702	0.00659	396	99.995
Sn #39 front	Pb	3982	0.0150	984	99.986
Sn #39 back	Pb	4714	"	1164	99.984
Sn #40 front	Pb	5169	0.0147	314	99.996
Sn #40 back	Pb	4974	"	302	99.996
Al #21 front	Fe	16204	0.0504	556	99.974
Al #21 front	Cu	11214	0.0943	139	
Al #21 back	Fe	13785	0.0504	473	99.978
Al #21 back	Cu	9715	0.0943	121	

Table 12: Filter Material Examined for X-ray Transmission Uniformity

Sample	Nominal t, mm	kV Used	Exposure time, min	Optical Density
Sn39	0.5	100	17	0.90
Sn40	0.5	100	35	1.53
Cu21	0.5	100	6	1.56
Cu01	1.0	100	12	0.95
Cu02	1.0	100	20	1.49
Cu42	0.15	60	10	1.84
Cu52	0.1	60	8	1.88
Cu72	0.01	30	5	1.05
Cu73	0.01	30	10	1.70
Cu74	0.01	30	10	2.19
Al01	2.0	100	1.5	1.57
Al11	1.0	60	4	1.90
Al21	0.5	30	13	0.83
Al31	0.1	30	5	1.96
Al52	0.05	30	6	2.61

Table 13a. Combinations of Pb Sheets Used for Required Thicknesses

Thickness Required, mm	ISO Technique	Combination	Thickness, mm	Percent Difference
5.5	LK240	27,32,34,30,6,1,29,12	5.4976	-0.04
5.0	NS300	10,7,19,26	4.9993	-0.01
3.5	LK210	21,4,17,28	3.4966	-0.10
3.0	NS250	9,14	2.9747	-0.84
1.5	LK170	22,15	1.4973	-0.18
1.0	NS200	18	1.0030	+0.30

Table 13b. Combinations of Sn Sheets Used for Required Thicknesses

Thickness Required, mm	ISO Technique	Combination	Thickness, mm	Percent Difference
6.5	WS300	40,24,18,27,33,25,11	6.5363	+0.56
4.0	LK125	9,13,22,12	4.0072	+0.19
4.0	WS250	23,15,7,17	4.0095	+0.24
3.0	LK170	8,31,37	2.9997	-0.00
3.0	NS200	30,10,14	2.9791	-0.70
3.0	NS300	35,29,20	2.9909	-0.30
2.5	NS150	39,6,19	2.5025	+0.10
2.0	NS250	21,34	2.0114	+0.57
2.0	WS200	26,38	2.0109	+0.55
2.0	LK100	5,16	2.0105	+0.53
2.0	LK210	4,36	2.0100	+0.50
2.0	LK240	28,32	2.0070	+0.35
1.0	NS120	2	1.0375	+3.75
1.0	WS150	3	1.0299	+2.99

Table 13c. Combinations of Cu Sheets Used for Required Thicknesses

Thickness Required, mm	ISO Technique	Combination	Thickness, mm	Percent Difference
5.0	NS100	3,6,7,8,37,50,48,68	4.9858	-0.28
5.0	NS120	19,20,13,10,29,46,42,52	4.9925	-0.15
3.0	HK280	1,2,9	3.0567	+1.89
2.5	HK300	21,23,40,24,63,55,71,70	2.5073	+0.29
2.5	LK70	22,25,33,38,39	2.6410	+5.64
2.0	NS80	11,12	2.0379	+1.90
2.0	NS200	15,16	2.0378	+1.89
2.0	WS110	5,18	2.0295	+1.48
1.6	HK250	28,30,27	1.5998	-0.01
1.2	LK55	26,32,57,79,73	1.1953	-0.39
1.15	HK200	44,14	1.1502	+0.01
1.0	LK170	17	1.0134	+1.34
1.0	LK125	4	1.0142	+1.42
0.60	NS60	49,54,80,43,76,60,65	0.6005	+0.08
0.50	WS80	34	0.5290	+5.80
0.50	LK210	36	0.5291	+5.82
0.50	LK240	41	0.5285	+5.70
0.50	LK100	82	0.5184	+3.68
0.30	WS60	67,53,66	0.2999	-0.04
0.25	LK35	51,59,77	0.2499	-0.06
0.21	NS40	64,56	0.2084	-0.75
0.18	LK30	47,74,72,75,78	0.1801	-0.07
0.15	HK100	45,81	0.1514	+0.93

Table 13d. Combinations of Al Sheets Used for Required Thicknesses

Thickness Required, mm	ISO Technique	Combination	Thickness, mm	Percent Difference
4.0	NS30	1,2	4.0818	+2.05
4.0	LK30	6,7	4.0786	+1.97
3.9	HK100	3,19,28,45,46,57	3.8969	-0.08
3.2	HK40	5,12,44	3.1977	-0.07
2.0	NS25	8	2.0409	+2.05
2.0	LK20	9	2.0412	+2.06
1.0	NS20	29,49,52,68,47,35,48	1.0030	+0.30
0.52	HK30	26	0.5201	+0.02
0.50	NS15	37,59,42,55,31,36	0.4974	-0.52
0.30	LK10	32,69,39,66	0.2998	-0.08
0.15	HK20	50,53	0.1500	+0.00
0.10	NS10	33	0.0997	-0.34

Figure 1. Sample Peak Fit and Integration

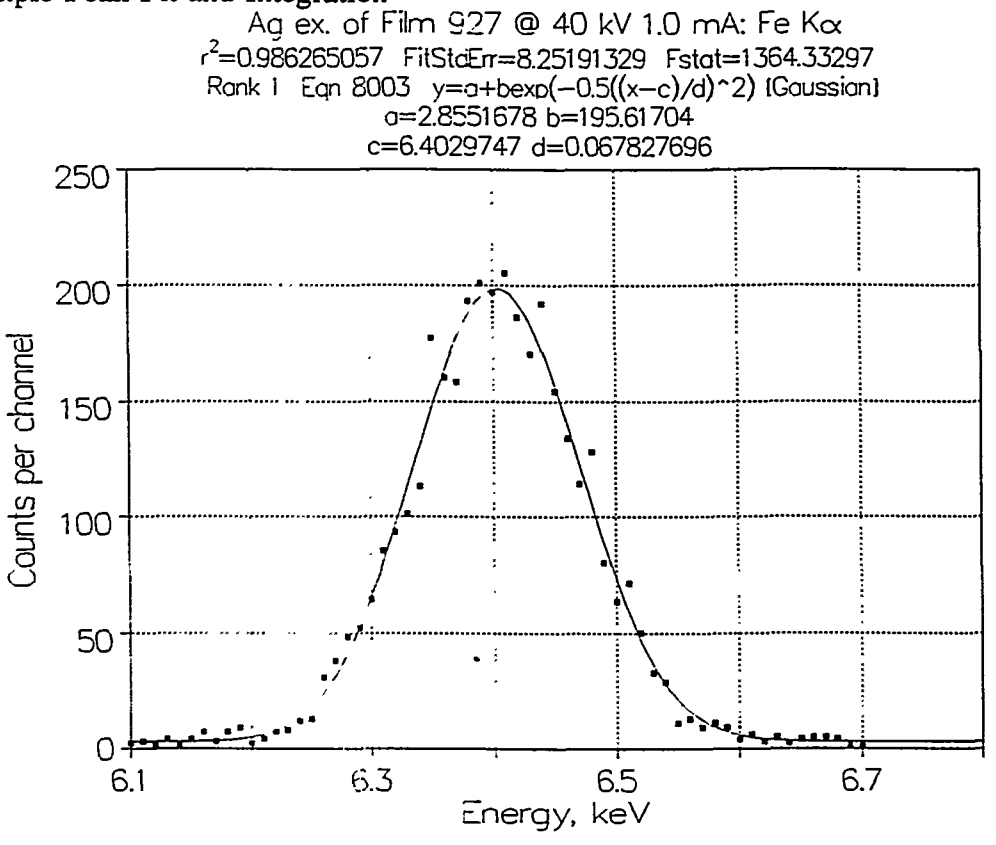


```
Ag ex. of Film 927 @ 40 kV 1.0 mA: Fe KÁ      Apr 15,1994 2:19 PM
61 Active X-Y Points
X: Energy, keV            Mean: 6.4           SD: 0.1775293403
Y: Counts per channel     Mean: 57.37704918   SD: 68.628265298
File Source: STANFE10.DAT

Rank 1  Eqn 8003  y=a+bexp(-0.5((x-c)/d)^2) [Gaussian]

r2 Coef Det     DF Adj r2       Fit Std Err     F-value
0.9862650566    0.9852839892    8.2519132888    1364.3329673

 Parm  Value          Std Error     t-value       95% Confidence Limits
 a     2.855167831    1.652330917   1.727963691   -0.45307574   6.1634114
 b     195.6170352    3.140375291   62.29097386   189.3294773   201.9045931
 c     6.402974707    0.001167022   5486.592935   6.400638133   6.40531128
 d     0.067827696    0.001420575   47.7466484    0.064983466   0.070671925
```

Integral from 6.1 keV to 6.7 keV = 3497.37
Function evaluated at 6.1 keV = 2.864
Function evaluated at 6.7 keV = 2.869
Background over 61 channels = 174.85
Net count total = 3322.28 counts

Figure 2. Iso-density Plot of Radiograph of Filter Cu21

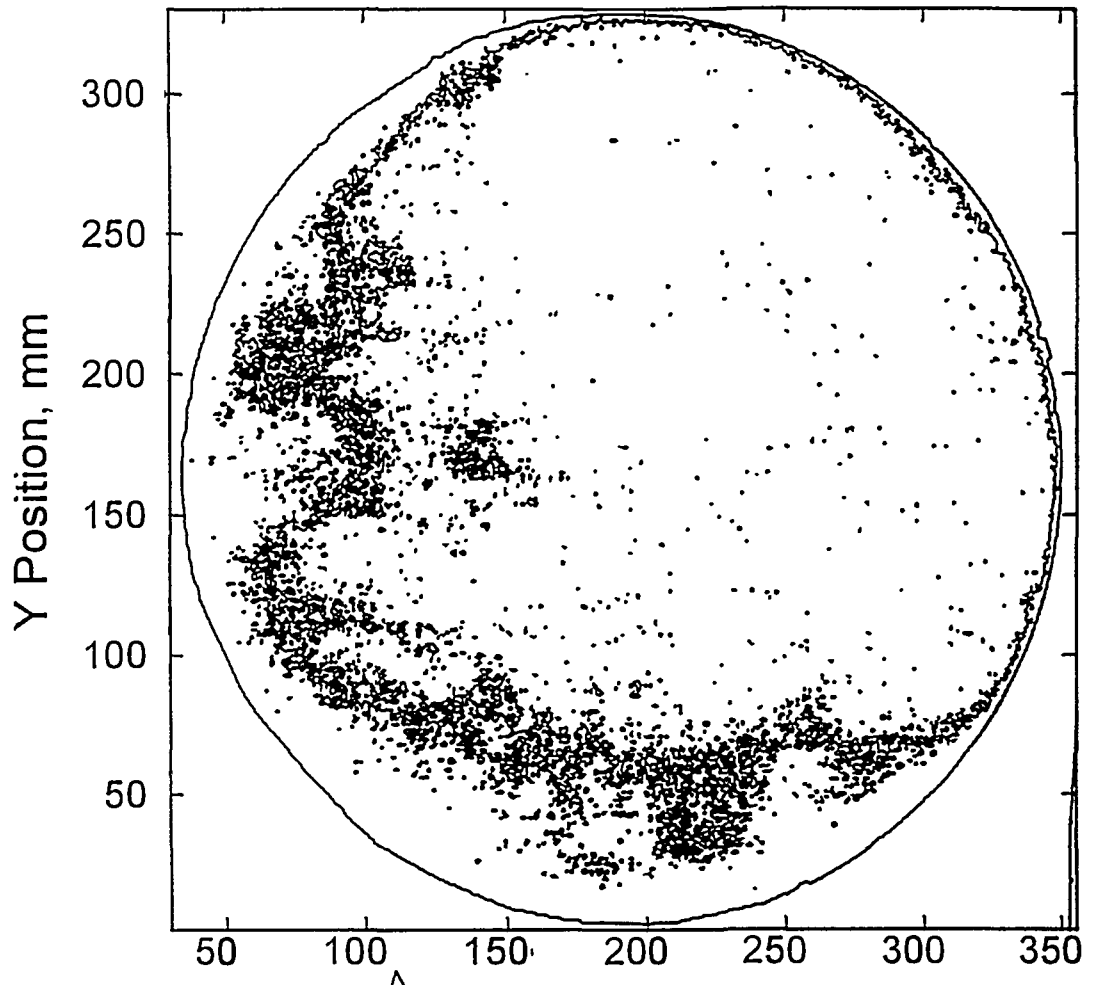

Contour levels at 1.45 and 1.545